ON THE FLOW VELOCITY OF THE ICE SHEET ALONG THE TRAVERSE ROUTE FROM SYOWA TO MIZUHO STATIONS, EAST ANTARCTICA

Kazuo SHIBUYA

National Institute of Polar Research, 9-10, Kaga 1-chome, Itabashi-ku, Tokyo 173

and

Kiyoshi ITO

Regional Observation Center for Earthquake Prediction, Faculty of Science, Kyoto University, Nasahara 944, Takatsuki 569

Abstract: The 21st Japanese Antarctic Research Expedition (JARE-21, 1979–1981) made several explosion seismic experiments by installing seismic stations along the S-H-Z route from Syowa to Mizuho Stations, on which JARE-14 (1972–1974) had made the traverse survey. Most of the seismic stations were selected to be closely located near the traverse stations, so that the position of each traverse station could be determined from that of a nearby seismic station determined by the NNSS positioning. By comparing the positions of selected traverse stations thus determined in 1980 with those determined in 1973, the flow velocity of the ice sheet along the S-H-Z route was estimated. Since the method of positioning and the referred geodetic coordinates by JARE-21 were not identical with those by JARE-14, several assumptions were made in the data reduction procedure and in the estimate of the flow velocity. The obtained magnitude of flow in 1973–1980 ranges from 108 m with 290° flow direction at S27-3 to 475 m with 267° flow direction at Z2 with the uncertainty of at most $\pm 14\%$ for the flow value and $\pm 13°$ for the flow direction. The change of the height at each traverse station ranges from -3.5 m at H17 to $+8.8$ m at H253 with about 10 m uncertainty. Topographical features of the obtained flow velocity are discussed in view of the comparison with previously obtained flow velocity, the flow lines deduced from the surface topography, the strain field measured near the route and the free-air gravity anomalies over the Mizuho Plateau.

1. Introduction

In the seven-year project "Glaciological Studies in Mizuho Plateau, East Antarctica, 1969–1975", JARE-14 (1972–1974) made a traverse survey along the S-H-Z route by installing 109 traverse poles over the 280 km distance from Syowa Station to Mizuho Station (NARUSE and YOKOYAMA, 1975). Most of the traverse stations have been maintained since by oversnow traverse parties between the two Stations every year, though the positioning has never been made until 1980. Seven years after the above traverse survey, JARE-21 (1979–1981) made several explosion seismic experiments in order to obtain the crustal velocity structure beneath the Mizuho Plateau as part of the three-year project, "Geophysical Investigations of the Crust and Upper-Mantle Structure around Syowa Station, East Antarctica", by installing 27 seismic stations along the same route (IKAMI *et al.*, 1982).

The seismic stations were so selected that they were closely located near some of the traverse stations settled by JARE-14 and the positioning was made utilizing NNSS satellites (SHIBUYA *et al.*, 1982). In this way, the positioning of the nearby traverse stations could be made. From the change of the positions of the traverse stations in 7 years, we can obtain the flow velocity of the ice sheet along the S-H-Z route. However, because of the differences between the positioning method and the reference ellipsoid adopted by JARE-14 and -21, careful procedures of data reduction are necessary. The coordinate transformations and datum shift are required before the comparison of the position in 1973 (hereafter referred to as the starting point S) with that in 1980 (referred to as the end point E). After the above corrections on the data of S, surface distance and direction between S and E were calculated to obtain the flow velocity on the surface under an assumption of a constant flow rate. The positioning of S has a corresponding error in the traverse survey, while that of E has a corresponding error in the satellite Doppler positioning. The influence of the above errors on the flow velocity was discussed.

2. Coordinate Transformation and Datum Shift

JARE-14 started the traverse survey from the astronomical station at Syowa Station. The geodetic latitude, the longitude and the elevation from mean sea level (m.s.l.) of the traverse station were calculated on the Bessel's reference ellipsoid. On the other hand, JARE-21 made the positioning of the seismic station using a two-wave NNSS receiver, JMR-1. The geodetic latitude, the longitude and the antenna height at the seismic station were obtained on the WGS-72 reference ellipsoid. In order to determine the transformation parameters between these different coordinate systems, receiving experiments of NNSS satellites were carried out at the astronomical station at Syowa Station. Results of the experiments are shown in Fig. 1, which is a reproduction of Fig. 6 of our previous paper (SHIBUYA *et al.*, 1982). Point A_3 is the most probable three-dimensional positioning of the astronomical station A due to the NNSS positioning method. The coordinate values of point A_3 and point A are summarized in Table 1, together with the corresponding errors in the positioning. As shown in Fig. 1, point A_3 has a shift of about 370–400 m toward a west-northwest direction against point A. The difference between the antenna height and the elevation from m.s.l. remained 31 ± 2 m. This is considered to show an approximate geoid height at the astronomical station. The above inconsistence between points A_3 and A can be attributed to the overall effects of the deflection of plumbline, the error in the satellite positioning and the inaccuracies of the astronomical positioning.

The relative location of the WGS-72 reference ellipsoid against the Bessel's reference ellipsoid in the region concerned is schematically illustrated in Fig. 2. Let us derive the transformation parameters using this figure after the formulation by HEISKANEN and MORITZ (1967). Assume a rectangular coordinate system XYZ whose origin agrees with the earth's center of gravity, the axes being directed as illustrated in Fig. 2. Let the coordinate of the center of the Bessel's ellipsoid with respect to XYZ system be $x_\circ$, $y_\circ$ and $z_\circ$. Then, the transformation formulas between the geodetic coordinates (ϕ, λ, h) and the rectangular coordinates (X, Y, Z) of a point outside the

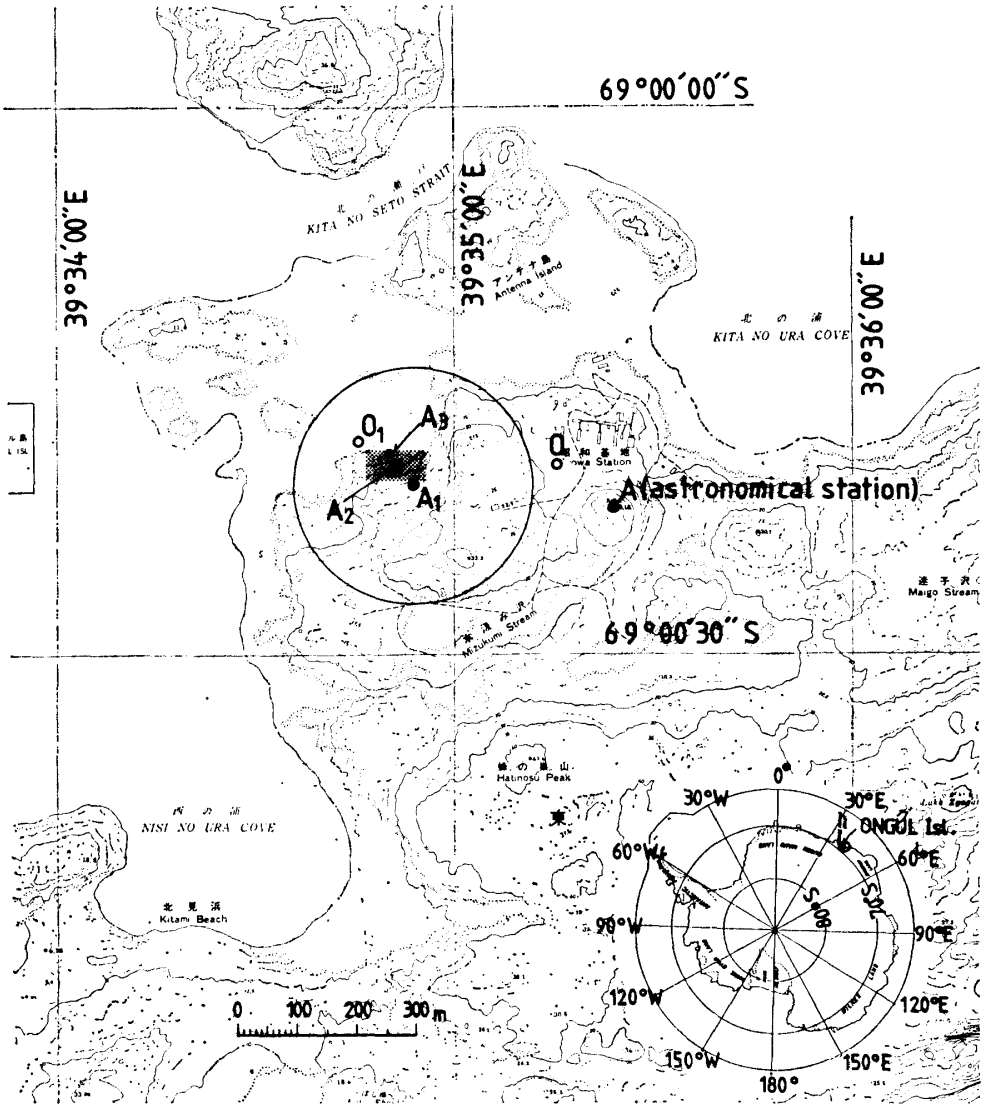

Fig. 1. Results of the NNSS positioning of the astronomical station at Syowa Station, reproduced from SHIBUYA et al. (1982). A_1 indicates a most probable two-dimensional fixing of point A by the one-wave receiver, JLE-3300B, and the open circle gives the standard deviation area of 200 m radius. A_2 indicates a most probable two-dimensional fixing of point A by the two-wave receiver, JMR-1, and the shaded box gives its standard deviation area. A_3 indicates a most probable three-dimensional fixing of point A, the positioning uncertainties of which are summarized in Table 1.

ellipsoid can be given by eq. (1).

$$\begin{aligned} X &= x_0 + (N+h)\cos\phi\cos\lambda, \\ Y &= y_0 + (N+h)\cos\phi\sin\lambda, \\ Z &= z_0 + \left(\frac{b^2}{a^2}N+h\right)\sin\phi. \end{aligned} \tag{1}$$

The notations above and hereafter are summarized in Table 2. If the coordinates of

Table 1. Coordinate values of the astronomical station at Syowa Station and the configuration parameters of Bessel's and WGS-72 standard ellipsoids.

	A (on the Bessel's ellipsoid)	A_s (on the WGS-72 ellipsoid)
Latitude	$\phi_B=69°00'20.0''S\pm4''$	$\phi_W=69°00'18.93''S\pm20$ m
Longitude	$\lambda_B=39°35'24.0''E\pm12''$	$\lambda_W=39°34'50.83''E\pm10$ m
Height	$h_B=29.18$ m (above m.s.l.)	$h_W=62.3$ m±5 m (antenna height)
Equator radius	$a_B=6377397.155$ m	$a_W=6378135$ m
Flattening	$f_B=1/299.152813$	$f_W=1/298.26$
$\delta\phi=\phi_W-\phi_B=-1.07''$	$\delta\lambda=\lambda_W-\lambda_B=-33.17''$	$\delta h=h_W-h_B=33.1$ m
$\delta a=a_W-a_B=738$ m	$\delta f=f_W-f_B=1.00062\times10^{-5}$	

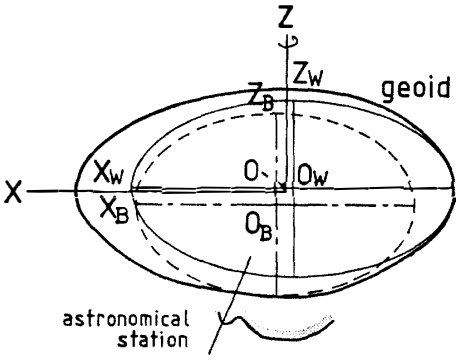

Fig. 2. Schematic location of the Bessel's and the WGS-72 reference ellipsoids in the region concerned. Taking the center of earth's gravity as O, Z axis is directed parallel to the axis of rotation. The center of the WGS-72 and the Bessel's reference ellipsoids, O_W and O_B, may be slightly offset against O. The axes Z_W and Z_B are parallel to the Z axis. Positive direction of the Y axis is perpendicular to the figure sheet.

the center of the ellipsoid are shifted by a small translation of $(\delta x_\circ, \delta y_\circ, \delta z_\circ)$, the configuration parameters (a, f) are altered by a small amount $(\delta a, \delta f)$, and the geodetic coordinates (ϕ, λ, h) are changed by also a small amount $(\delta\phi, \delta\lambda, \delta h)$, respectively, then the rectangular coordinates (X, Y, Z) are changed as follows when higher-order terms in Taylor's expansion are neglected:

$$\begin{aligned}
\delta X&=\delta x_\circ+(\partial X/\partial a)\delta a+(\partial X/\partial f)\delta f+(\partial X/\partial\phi)\delta\phi+(\partial X/\partial\lambda)\delta\lambda+(\partial X/\partial h)\delta h,\\
\delta Y&=\delta y_\circ+(\partial Y/\partial a)\delta a+(\partial Y/\partial f)\delta f+(\partial Y/\partial\phi)\delta\phi+(\partial Y/\partial\lambda)\delta\lambda+(\partial Y/\partial h)\delta h,\\
\delta Z&=\delta z_\circ+(\partial Z/\partial a)\delta a+(\partial Z/\partial f)\delta f+(\partial Z/\partial\phi)\delta\phi+(\partial Z/\partial\lambda)\delta\lambda+(\partial Z/\partial h)\delta h.
\end{aligned}\tag{2}$$

Substitution of all the partial derivatives of eq. (1) into eq. (2) finally yields

$$\begin{aligned}
\delta X&=\delta x_\circ-a\sin\phi\cos\lambda\delta\phi-a\cos\phi\sin\lambda\delta\lambda+\cos\phi\cos\lambda(\delta h+\delta a+a\sin^2\phi\delta f),\\
\delta Y&=\delta y_\circ-a\sin\phi\sin\lambda\delta\phi+a\cos\phi\cos\lambda\delta\lambda+\cos\phi\sin\lambda(\delta h+\delta a+a\sin^2\phi\delta f),\\
\delta Z&=\delta z_\circ+a\cos\phi\delta\phi+\sin\phi(\delta h+\delta a+a\sin^2\phi\delta f)-2a\sin\phi\delta f.
\end{aligned}\tag{3}$$

Details of the derivations are in the above reference (p. 204–208).

Since the position of the astronomical station at Syowa Station remains unchanged in XYZ space, the translation $\delta x_\circ$, $\delta y_\circ$ and $\delta z_\circ$ can be obtained by letting $\delta X=\delta Y=\delta Z=0$ in eq. (3) and expressing in terms of $(\delta a, \delta f)$ and $(\delta\phi, \delta\lambda, \delta h)$ as follows:

$$\begin{aligned}
\delta x_\circ&=a\sin\phi\cos\lambda\delta\phi+a\cos\phi\sin\lambda\delta\lambda-\cos\phi\cos\lambda(\delta h+\delta a+a\sin^2\phi\delta f),\\
\delta y_\circ&=a\sin\phi\sin\lambda\delta\phi-a\cos\phi\cos\lambda\delta\lambda-\cos\phi\sin\lambda(\delta h+\delta a+a\sin^2\phi\delta f),\\
\delta z_\circ&=-a\cos\phi\delta\phi-\sin\phi(\delta h+\delta a+a\sin^2\phi\delta f)+2a\sin\phi\delta f.
\end{aligned}\tag{4}$$

Table 2. List of notations and expressions for Θ_1, Θ_2 and Θ_3.

a	equator radius of a reference ellipsoid
B	denotes the suffix which means Bessel's reference ellipsoid
b	polar radius of a reference ellipsoid
E	denotes the position of the traverse station in 1980 measured by JARE-21
e	first eccentricity $\sqrt{a^2-b^2}/a$
e'	second eccentricity $\sqrt{a^2-b^2}/b$
f	flattening $(a-b)/a$
g_{obs}	observed gravity value in milligal at each measuring station
h	height above m.s.l. or antenna height in meters
I	ice thickness in meters at each measuring station by radio-echo sounding
l	distance between S and E, see Fig. 4
N	radius of curvature in the prime vertical, $a^2/(a^2\cos^2\phi+b^2\sin^2\phi)^{1/2}$
r	radial offset of the seismic station against the traverse station, see Fig. 3
S	denotes the position of the traverse station in 1973 measured by JARE-14
$\sin\theta_s$	slope of the surface features of the ice sheet in eq. (10)
t	$\tan\phi$
V	$(1+e'^2\cos^2\phi)^{1/2}$
V_s	surface velocity of the ice sheet in meter per year
W	denotes the suffix which means WGS-72 reference ellipsoid
X,Y,Z	rectangular coordinates whose origin is the earth's center of gravity
x_o,y_o,z_o	translation of the center of a reference ellipsoid with respect to the XYZ coordinates system
α_{ES}	azimuth from E to S, see Fig. 4
α_{SE}	azimuth from S to E, see Fig. 4
γ_o	normal gravity in milligal as a function of latitude
Δg_o	free-air anomaly in milligal
$\Delta g_o''$	Bouguer anomaly in milligal
ΔH	elevation minus ice thickness, that is, bedrock elevation in meter
δ	denotes the lateral change of Δg, h and ΔH
ϕ	geodetic latitude
λ	geodetic longitude
η^2	$e'^2\cos^2\phi$
θ	azimuth of the seismic station against the traverse station measured from geographic north, see Fig. 3
Θ_1	$\Delta\phi^2(3\eta^2-6\eta^4+9\eta^6-3t^2\eta^2+21t^2\eta^4-54t^2\eta^6)/24+\cos^2\phi\Delta\lambda^2(-2-3t^2+3t^2\eta^2-3t^2\eta^4+3t^2\eta^6)/24+\Delta\phi^4(-36\eta^2+207\eta^4+36t^2\eta^2-1062t^2\eta^4+135t^4\eta^4)/5760+\Delta\phi^2\cos^2\phi\Delta\lambda^2(-16-60t^2+4\eta^2-4\eta^4+102t^2\eta^2+48t^2\eta^4+90t^4\eta^2-630t^4\eta^4)/5760+\cos^4\phi\Delta\lambda^4(-8-20t^2+15t^4-8\eta^2+96t^2\eta^2-15t^4\eta^2+15t^4\eta^4)/5760$
Θ_2	$\Delta\phi^2(1-\eta^2+\eta^4-\eta^6-9t^2\eta^2+18t^2\eta^4-27t^2\eta^6)/24+\cos^2\phi\Delta\lambda^2(-t^2)/24+\Delta\phi^4(7+10\eta^2-27\eta^4-54t^2\eta^2-642t^2\eta^4+675t^4\eta^4)/5760+\Delta\phi^2\cos^2\phi\Delta\lambda^2(-16-70t^2-158t^2\eta^2+158t^2\eta^4+90t^4\eta^2-180t^4\eta^4)/5760+\cos^4\phi\Delta\lambda^4(-24t^2+3t^4-24t^2\eta^2)/5760$
Θ_3	$\Delta\phi^2(3+2\eta^2-2\eta^4+2\eta^6)/24+\cos^2\phi\Delta\lambda^2(2+2\eta^2)/24+\Delta\phi^4(75-4\eta^2+92\eta^4-120t^2\eta^2+264t^2\eta^4)/5760+\Delta\phi^2\cos^2\phi\Delta\lambda^2(60-120t^2+52\eta^2-320t^2\eta^2-112t^2\eta^4)/5760+\cos^4\phi\Delta\lambda^4(48-24t^2+96\eta^2-48\eta^4-120t^2\eta^2-96t^2\eta^4)/5760$

After δx_o, δy_o and δz_o are estimated, the correction terms which transform the geodetic coordinates on one reference ellipsoid to another can be obtained by letting $\delta X=\delta Y=\delta Z=0$ and solving eq. (3) for $\delta\phi$, $\delta\lambda$ and δh, respectively.

$$\begin{aligned}
\delta\phi &= \sin\phi\cos\lambda\frac{\delta x_0}{a} + \sin\phi\sin\lambda\frac{\delta y_0}{a} - \cos\phi\frac{\delta z_0}{a} + 2\sin\phi\cos\phi\delta f,\\
\delta\lambda &= -\frac{\sin\lambda}{\cos\phi}\frac{\delta x_0}{a} - \frac{\cos\lambda}{\cos\phi}\frac{\delta y_0}{a},\\
\frac{\delta h}{a} &= -\cos\phi\cos\lambda\frac{\delta x_0}{a} - \cos\phi\sin\lambda\frac{\delta y_0}{a} - \sin\phi\frac{\delta z_0}{a} - \frac{\delta a}{a} + \sin^2\phi\delta f.
\end{aligned} \tag{5}$$

3. Data Reduction and the Results

Table 3 shows a part of the traverse survey data by JARE-14. Columns 1 and 2 give the route station numbers and the corresponding traverse station numbers, respectively. Though the traverse survey was further proceeded from Z2 to Mizuho Station, no comparison was carried out for further traverse stations because the geodetic control at Mizuho Station was found unsatisfactory for the estimate of ice flow as will be discussed later. Columns 3, 4 and 5 give the geodetic coordinates on the Bessel's reference ellipsoid, where the height means the elevation from m.s.l., all of which are compiled from Table 2 of the paper by NARUSE and YOKOYAMA (1975). It is noted that S27-3 which corresponds to the seismic station ST3 was not a traverse station and the geodetic coordinates were interpolated from those of S26-5 (T015) and S28-1 (T016). Substituting the configuration parameters of the Bessel's reference ellipsoid, the corresponding geodetic coordinate values of point A and the differences $\delta\phi$, etc. in Table 1 into eq. (4), the translation of the center of the WGS-72 reference ellipsoid from that of the Bessel's reference ellipsoid in the region concerned can be estimated as

$$\delta x_0 = -552 \text{ m},\ \delta y_0 = 42 \text{ m and } \delta z_0 = 623 \text{ m}. \tag{6}$$

Table 3. The location of traverse stations in 1973 and the correction terms from Bessel's to WGS-72 coordinates.

Route station	Traverse station	Latitude ϕ_B	Longitude λ_B	Elevation h_B	$\delta\phi$	$\delta\lambda$	λh
S22-1	T011	69°01′35″	40°19′55″	764 m	2.6″	−33.4 m	31.7 m
S27-3		69 02 28	40 35 08	930	2.6	−33.6	31.1
H17	T019	69 05 09	40 47 57	1035	2.5	−33.8	30.6
H48-1	T024	69 08 42	40 57 17	1133	2.5	−34.0	30.1
H74-1	T028	69 12 49	41 07 24	1207	2.5	−34.2	29.6
H155	T045	69 30 01	41 47 28	1465	2.5	−35.0	27.7
H174	T048	69 34 08	41 57 18	1524	2.5	−35.2	27.2
H194	T052	69 38 22	42 08 02	1560	2.5	−35.4	26.7
H213	T056	69 42 33	42 17 57	1617	2.5	−35.6	26.2
H231	T059	69 46 26	42 27 37	1667	2.5	−35.9	25.8
H253	T064	69 51 16	42 38 49	1739	2.5	−36.1	25.2
H272	T068	69 55 09	42 49 45	1789	2.5	−36.3	24.7
Z2	T076	70 02 90	43 11 05	1926	2.5	−36.7	23.8

The correction terms from the Bessel's coordinate values to the WGS-72 coordinate values at each traverse station can be obtained by substituting the translations in eq. (6) and the corresponding geodetic coordinate values in Table 3 into eq. (5). Columns 6, 7 and 8 summarize such correction terms for the latitude, the longitude and the an-

Table 4. The location of seismic stations in 1980 and the correction terms to deduce the corresponding traverse station from the seismic station on WGS-72 coordinates.

Seismic station	Traverse station	Pass number	Latitude ϕW	Longitude λW	Antenna height hW	r	θ	$\delta'\phi$	$\delta'\lambda$	$\delta'h$
ST2	T011	4	69°01′35.1″	40°18′46.2″	776.5 m	126 m	19 deg	−3.8″	3.7″	—
3		3	69 02 33.1	40 34 31.6	950.8	135	329	−3.7	−6.3	—
4	T019	8	69 05 06.9	40 47 17.3	1062.6	0	0	0.0	0.0	−0.5
5	T024	3	69 08 41.0	40 56 34.6	—	0	0	0.0	0.0	−0.5
6	T028	2	69 12 48.6	41 06 35.6	(1236.6)	0	0	0.0	0.0	—
10	T045	3	69 29 56.3	41 46 31.0	1501.8	52	47	−1.1	3.5	−2.9
11	T048	3	69 34 05.9	41 56 33.9	1495.3	49	45	−1.1	3.2	−2.9
12	T052	3	69 38 17.4	42 07 09.8	1562.0	20	85	−0.1	1.9	−2.9
13	T056	*6	69 42 30.1	42 17 02.5	1666.9	40	43	−0.9	2.5	−2.9
14	T059	12	69 46 22.7	42 26 26.6	1695.1	70	85	−0.2	6.5	−2.9
15	T064	10	69 51 14.8	42 37 35.3	1775.9	73	60	−1.2	5.9	−2.9
16	T068	4	69 55 08.0	42 48 30.1	1824.3	34	80	−0.2	3.1	−2.9
18	T076	10	70 02 13.4	43 09 37.3	1952.0	73	63	−1.1	6.2	−2.9
27	T109	17	70 42 03.8	44 17 37.8	2261.1	49	340	−1.5	−1.6	−2.9

tenna height, respectively. The corrected $\phi_B + \delta\phi$, $\lambda_B + \delta\lambda$ and $h_B + \delta h$ in each row of Table 3 give the presumed position of each traverse station on the WGS-72 reference ellipsoid in 1973, to be listed in Table 5. It is noted that the addition of δh (column 8) to the elevation h from m.s.l. (column 5) gives an approximate antenna height on the assumption of constant geoid height of 33.1 m over the region concerned.

Table 4 shows a part of the list of the seismic stations by JARE-21. Columns 1 and 2 give the seismic station numbers and the corresponding traverse station numbers, respectively. We could not find poles for the positioning at two traverse stations which correspond to ST1 (S16) and ST17 (H295-1) in 1980. As for seismic stations ST7, ST8 and ST9, there were nearby traverse stations T033 (H93), T037 (H113-1) and T042 (H137), respectively. However, the above traverse stations were the newly installed ones by JARE-18 (1976–1978) after the traverse poles by JARE-14 were found entirely buried under snow. The offsets of the position between JARE-14 and JARE-18 are not known and the estimate of flow velocity at these traverse stations was abandoned.

Column 3 indicates the number of satellite passes used in the NNSS positioning. When the pass number is less than 3, it often occurs that three-dimensional fixing cannot be obtained. In that case, two dimensional fixing is applied assuming the pre-fixed antenna height at the corresponding station. A star in column 3 indicates that, though the pass number was less than 3 in a tight mode, appropriate three-dimensional positioning could be obtained in a loose mode by allowing passes with higher angle elevation (70°∼80°) at the closest approach. Since convergent procedures of the NNSS positioning in the antarctic region were examined taking the pass number as a parameter (SHIBUYA *et al.*, 1982), the positioning error at each station can be estimated by referring to this column.

Columns 4, 5 and 6 in Table 4 indicate the geodetic latitude, the longitude and the antenna height, respectively. Since the seismic stations were settled a little distant from the traverse stations as illustrated in Fig. 3 for a case at S22-1 (T011) as an example,

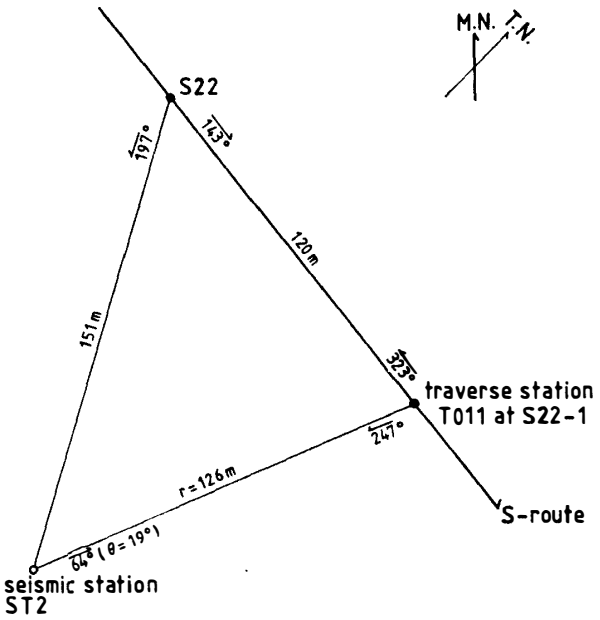

Fig. 3. The seismic station is slightly offset from the traverse station with radial distance r and the azimuth θ. The azimuth was measured by the hand-bearing compass and is reduced to geographic azimuth in Table 4.

the offset between the two positions should be accounted for. Columns 7 and 8 show the radial offset r and the azimuth θ measured from geographic north of the seismic station against the traverse station (see also Fig. 3). The offset correction can be calculated using Puissant's formula (BOMFORD, 1980) and the position of individual traverse station can be deduced from the position of corresponding seismic station by the correction terms in columns 9 and 10 for geodetic latitude and the longitude, respectively. In order to reduce the antenna height at the receiving point to that at the traverse station, the height from the earth's surface to the electric center of the receiving antenna and the effect of surface topography have to be corrected. The height of electric center changed from 0.5 to 2.9 m after ST8 (see column 11 in Table 4), as the receiving antenna was set on the roof (2.3×4.4 m area) of the oversnow vehicle. The effect of the declination of surface topography on the height correction is not considered here, since the slope of the ice sheet is negligibly small to yield significant height difference for the range of r (0–135 m) in Table 4.

Table 5 shows the positions of each traverse station in 1973 and 1980 which were deduced by procedures as described above referring to the WGS-72 ellipsoid. The geodetic latitude ϕ_S of each traverse station in 1973 in column 3 changed to that ϕ_E in 1980 in column 4. Likewise, columns 5 and 6 and columns 7 and 8 show pairs of the

Table 5. Change of the geodetic coordinates of the traverse stations in 7 years from 1973 to 1980.

Route station	Traverse station	Latitude in 1973 ϕ_S	Latitude in 1980 ϕ_E	Longitude in 1973 λ_S	Longitude in 1980 λ_E	Height in 1973 h_S	Height in 1980 h_E
S22-1	T011	69°01′37.6″S	69°01′31.3″S	40°19′21.6″E	40°18′49.9″E	795.7 m	—
S27-3		69 02 30.6	69 02 29.4	40 34 34.4	40 34 25.3	961.1	950.8 m
H17	T019	69 05 11.5	69 05 06.9	40 47 23.2	40 47 17.3	1065.6	1062.1
H48-1	T024	69 08 44.5	69 08 41.0	40 56 43.0	40 56 34.6	1163.1	—
H74-1	T028	69 12 51.5	69 12 48.6	41 06 49.8	41 06 35.6	1236.6	(1236.6 fix)
H155	T045	69 30 03.5	69 29 55.2	41 46 53.0	41 46 34.5	1492.7	1498.9
H174	T048	69 34 10.5	69 34 04.8	41 56 42.8	41 56 37.1	1551.2	1492.4
H194	T052	69 38 24.5	69 38 17.3	42 07 26.6	42 07 11.7	1586.7	1559.1
H213	T056	69 42 35.5	69 42 29.2	42 17 21.4	42 17 05.0	1643.2	1664.0
H231	T059	69 46 28.5	69 46 22.5	42 27 01.1	42 26 33.1	1692.8	1692.2
H253	T064	69 51 18.5	69 51 13.6	42 38 12.9	42 37 41.2	1764.2	1773.0
H272	T068	69 55 11.5	69 55 07.8	42 49 08.7	42 48 33.2	1813.7	1821.4
Z2	T076	70 02 11.5	70 02 12.3	43 10 28.3	43 09 43.5	1949.8	1949.1

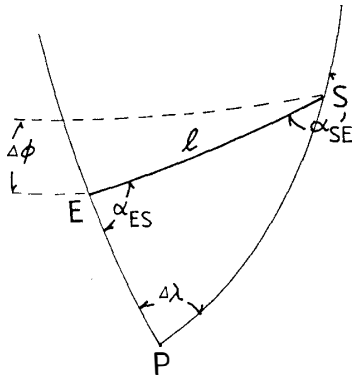

Fig. 4. Schematic drawing of the positional change of the traverse station, indicating the flow velocity vector. P denotes the south pole and P, S and E make a spherical triangle for the calculation of the total flow and the flow direction.

geodetic longitude and the antenna height of the traverse station in 1973 and in 1980, respectively. Figure 4 schematically illustrates the change $\Delta\phi=\phi_E-\phi_S$ and $\Delta\lambda=\lambda_E-\lambda_S$ of the traverse station. Since the starting point S and the end point E are now on the same reference ellipsoid, the distance l between S and E and the azimuth α_{SE} from S to E (measured from geographic north) give the vector of the surface flow at the station on the ice sheet in the last 7 years. The vector can be calculated from the changes of the geodetic latitude $\Delta\phi$ and the longitude $\Delta\lambda$, applying the fourth-order expansion of the Gauss' mid-latitude formula (HUBENY, 1959) as follows:

$$\begin{aligned} l\cos\alpha &= N\Delta\phi\ (\frac{1}{V^2}+\Theta_1), \\ l\sin\alpha &= N\cos\phi\Delta\lambda\ (1+\Theta_2), \\ \Delta\alpha &= t\cos\phi\Delta\lambda\ (1+\Theta_3), \end{aligned} \tag{7}$$

in which,

$$\begin{aligned} \Delta\phi &= \phi_E-\phi_S, \\ \Delta\lambda &= \lambda_E-\lambda_S, \\ \phi &= \frac{1}{2}\ (\phi_S+\phi_E), \\ \alpha &= \frac{1}{2}\ (\alpha_{SE}+\alpha_{ES}), \\ \Delta\alpha &= \alpha_{ES}-\alpha_{SE}. \end{aligned}$$

In eq. (7), Θ_1, Θ_2 and Θ_3 are expressed by a lengthy fourth-order polynominal of $\Delta\phi$ and $\Delta\lambda$, as are summarized in Table 2 and V is also given in the table. Substitution of the corresponding $\Delta\phi$ and $\Delta\lambda$ obtained from Table 5 into eq. (7) yields the flow for latitudinal direction $l\sin\alpha$ and that for longitudinal direction $l\cos\alpha$. Total surface flow l and the azimuth α_{SE} of the flow direction obtained are summarized together with the above directional components in columns 3–6 of Table 6. Assuming a constant flow rate, the flow velocity V_s at each station which is obtained by dividing the value of total flow vector l by 7.1 years' interval is given in column 8. The change of the height during

Table 6. Summary of the flow of ice sheet on the S-H-Z route in 1973–1980. Negative signs in columns 3 and 4 indicate southward and westward flow directions, respectively.

Route station	Traverse station	$l\sin\alpha$	$l\cos\alpha$	l	α_{SE}	Δh	V_s	Pass number
S22-1	T011	195.2 m	−351.9 m	402.4 m	299 deg	—	57 m/a	4
S27-3		37.2	−101.0	107.6	290	−10.3 m	15	3
H17	T019	142.5	−65.3	156.8	335	−3.5	22	8
H48-1	T024	108.5	−92.7	142.7	320	—	20	3
H74-1	T028	86.8	−158.5	180.7	299	—	26	2
H155	T045	257.2	−200.9	326.4	322	+6.2	46	3
H174	T048	176.6	−61.7	187.1	341	−58.8	26	3
H194	T052	223.1	−160.8	275.0	324	−27.6	39	3
H213	T056	195.2	−176.4	263.1	318	+20.8	37	*6
H231	T059	185.9	−300.2	353.1	302	−0.6	50	12
H253	T064	151.9	−338.6	371.1	294	+8.8	52	10
H272	T068	114.7	−378.0	395.0	287	+7.7	56	4
Z2	T076	−24.8	−474.4	475.0	267	−0.7	67	10

7.1 years or the vertical component of the flow vector is obtained by the difference $\Delta h = h_E - h_S$, as summarized in column 7.

4. Estimation of Errors

The estimate of errors in the total flow and the flow velocity depends on the errors in the positionings of both S and E. Since the method of positioning and the referred geodetic system were not identical between JARE-14 and JARE-21, it is rather difficult to estimate the errors accurately. As will be described later, uncertainty in the estimate of total flow is influenced by the angle between the flow direction and the route direction. We will discuss the effect of positioning errors for the representative values of total flow, flow direction and route direction, and the uncertainty areas in S and E will be estimated. The estimate is carried out by dividing the route into two portions, the first portion of S16-S30-H101 and the second portion of H101-H304-Z11.

JARE-14 made the traverse survey measuring the distance between the two traverse poles using mostly the electro-optical distance meter (Hewlett Packard 3800B) and measuring the azimuth by the theodlite (Wild T2). Though the traverse route was not closed and the survey was not always based on the Japanese standard operating procedure for the fourth-order triangulation, the geodetic control carried out at T035 (H101-1) gives us an appropriate estimate of accumulated positioning error there.

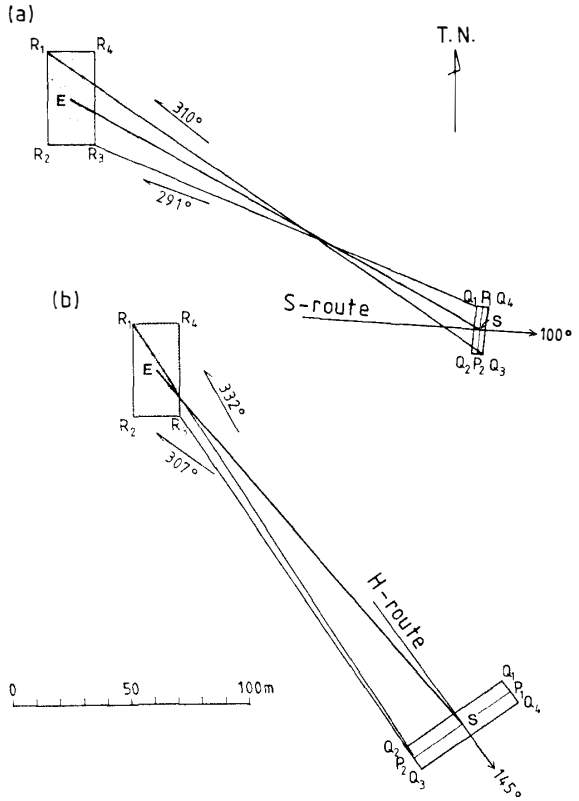

Fig. 5. Schematic illustration of the estimate of uncertainties in the total flow and the flow direction. (a) for the first portion S16-S30-H101, (b) for the second portion H101-H304-Z11. For details, see text.

Since T035 is located approximately one-third (80 km) from Syowa to Mizuho Stations along the S-H-Z route, the difference between the calculated azimuth from T035 to T036 and the observed one by the sunshot should give the error of the direction of traverse route and consequently of the positioning. Observed difference obtained by the sunshot was 15″ with a possible error of 6″. Therefore, the uncertainty in the perpendicular component against the route direction of the positioning of S is given by $SP_1=SP_2\sim 80\text{ km}\times 20''\sim 10$ m as schematically illustrated in Fig. 5a. If we consider 0.3×10^{-4} uncertainty of the measured distances by the electro-optical distance meter, the net accumulation of errors for the component parallel to the route direction can be estimated roughly as $80\text{ km}\times 3\times 10^{-5}\sim\pm 2.4$ m at each traverse station in the first portion of the route. Therefore the uncertainty area for S can be drawn by an open box $Q_1Q_2Q_3Q_4$ as schematically illustrated in Fig. 5a.

In contrast to the traverse survey, the error in the NNSS positioning does not transfer nor accumulate, but it depends on the received pass number. The absolute accuracy of NNSS positioning by the broadcasted ephemerides in the antarctic region can be estimated as a function of the pass number, for example as shown in Table 6 and Fig. 5 in our previous paper (SHIBUYA *et al.*, 1982). If we put the uncertainty-area of ± 20 m for the north-south direction and ± 10 m for the east-west direction against E, which is expressed by the shaded box $R_1R_2R_3R_4$ in Fig. 5a, variations of the representative total flow SE (200 m) and the flow direction (300°) are given by the ranges of the length and the direction of the line segments drawn between two boxes of uncertainty area with S and E as shown in this figure. From simple geometry, the minimum value of the total flow is $Q_1R_3\sim 176$ m, whereas the maximum is $Q_3R_1\sim 225$ m. Those values give uncertainty of about $\pm 12\%$ for the total flow. As for the flow direction, upper and lower limits of the variation are given by the direction of $\overrightarrow{Q_2R_4}\sim 310°$ and that of $\overrightarrow{Q_4R_2}\sim 291°$, respectively, which are approximately $\pm 10°$ around 300° of the representative flow direction. The area $Q_1Q_2Q_3Q_4$ should be smaller for a traverse station near Syowa Station; however, the area $R_1R_2R_3R_4$ would not be significantly small for the range of pass number used in the 1980 NNSS positionings as shown in Table 4. Then, the proportion of uncertainties in the total flow and flow direction becomes comparatively large when the value of total flow is small. Therefore, the uncertainties in the flow vector have some fluctuations according to the variations of the corresponding values of total flow, flow direction and route direction at each traverse station. We adopted, however, the above values $\pm 12\%$ and $\pm 10°$ as a representative uncertainty for the total flow value and that for the flow direction over the first portion of the route, respectively.

The estimate of errors in the second portion (H101-H304-Z11) can similarly be estimated from an example illustrated in Fig. 5b, with which the flow value $SE=200$ m, the flow direction 320° and the route direction 145°. The geodetic control at T080 (Z11-1), which is located about two-thirds (180 km) from Syowa to Mizuho Stations along the S-H-Z route, showed the difference of 23″ between the observed and the calculated azimuth from T080 to T079. Considering 6″ error in the sunshot, the possible error in the positioning of S for the perpendicular component to the route direction is, in this case, $SP_1=SP_2\sim 180\text{ km}\times(23''+6'')\sim 25$ m. Together with the uncertainty of $180\text{ km}\times 3\times 10^{-5}\sim 6$ m for the route direction, the box $Q_1Q_2Q_3Q_4$ in Fig. 5b can

be considered as the uncertainty area with S. The uncertainty area with E can also be illustrated by the same size of the box as that in Fig. 5a. Similar geometrical analysis gives $\pm 14\%$ uncertainty for the total flow from $Q_2R_3 \sim 172$ m to $Q_3R_1 \sim 228$ m and $\pm 13°$ uncertainty for the flow direction from $\overrightarrow{Q_1R_2} \sim 307°$ to $\overrightarrow{Q_2R_4} \sim 332°$ on the second portion of the route, respectively. Those values of uncertainties in the flow vector could be taken as representative for the second portion of the route.

In order to estimate the flow value on the remaining route of Z11-Mizuho Station accurately, the accumulated azimuthal error at Mizuho Station has to be smaller than 1′. However, partly because of bad weather at the time of the traverse survey, geodetic control at Mizuho Station showed such a large discrepancy as 20′12″ between the observed and the calculated azimuth from T109 (Mizuho Station) to T108. Therefore, the estimates of the flow vector on the last portion by the same procedures as above were abandoned in this paper.

The apparent change of the antenna height Δh in column 7 of Table 6 is as large as -59 m at H174 or $+21$ m at H213. However, since the uncertainty of height determination in the NNSS positioning is greater than 10 m when the pass number is less than 7 in a tight mode (SHIBUYA *et al.*, 1982) or it is not estimated in the receiving conditions in a loose mode, reliable range of the values of Δh in Table 6 may be only from -3.5 m at H17 to $+8.8$ m at H253. The actual height change of the traverse station in 7.1 years should include those caused by the downward velocity of the ice sheet, downward component of the surface declination, accumulation and/or ablation of snow layers. It is therefore difficult to deduce vertical component of the flow only from the change of antenna height. For such a purpose, measurements of regional variations in the accumulation or ablation of snow layers as well as more accurate determination of the antenna height are required.

5. Discussion

To know the pattern of flow of the ice sheet is one of the important keys for the estimate of mass balance of Antarctic ice sheet. The direction of flow is related with the bedrock morphology as well as with the surface topography of the ice sheet. Figure 6 is a reproduction of Fig. 33 of a paper by NARUSE (1978) on which the flow vectors obtained in the present study are added at its right upper part. According to NARUSE (1978), flow lines along the A-route (approximately on 2600 m elevation contour) were drawn parallel to flow vectors determined by the deformation of strain grids settled on the route. Flow lines in other regions were drawn as they were normal to the surface contour lines. Directions of flow along the traverse route in the Sôya drainage basin obtained in this study are almost parallel with or slightly deviated from the direction of the flow line determined from the surface topography.

There are several observations of the strain rate carried out at various sites of single strain grid as at S40, S100, S160, etc. as can be seen in Fig. 6. If the strain condition at S40 (near ST5) is the same as that at ST5 (H48-1) on the S-H-Z route, the direction of flow should coincide with the principal axis of strain. The former is 320° (see Table 6 in this paper) whereas the latter is 340° (see Table 2 of NARUSE and SHIMIZU, 1978), which results in the difference of 20°. Similar comparison between the direction

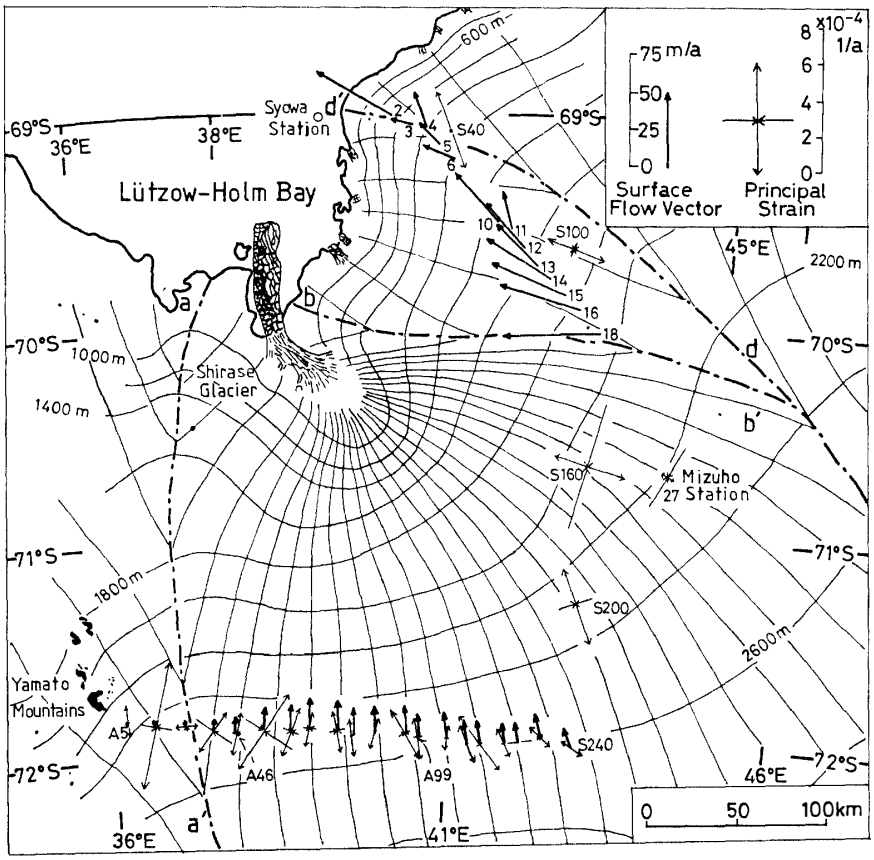

Fig. 6. Flow velocities on the S-H-Z route superposed onto flow lines over the Mizuho Plateau by NARUSE *(1978), reproduction from Naruse's paper with the author's courtesy.*

of the flow velocity at ST14 (H231), 302°, and that of the principal axis of strain at S100, 289°, gives 13° discrepancy. The coincidence between the direction of flow and the principal strain axis within 20° on the first and second portions of the S-H-Z route may support an inference that the direction of flow velocity is close to that of the principal axis of strain in the tensile field of large positive dilatation proposed by NARUSE (1978).

Figure 7 is a reproduction of the free-air anomaly map by ABE *et al.* (1978) on which the surface flow velocities in Fig. 6 are superposed. The contour lines in the map give the distribution of

$$\Delta g_o = g_{obs} + 0.3086\, h - \gamma_o, \tag{8}$$

where h is elevation from m.s.l.

On the assumption of insignificant lateral changes of the Bouguer anomaly, where

$$\Delta g_o'' = g_{obs} + 0.3086\, h - 0.1119\, h + 0.0742\, I - \gamma_o, \tag{8}'$$

the lateral change of the free-air anomaly can be related to the bedrock relief as

$$\delta(\Delta g_o) \sim 0.0377[\delta h + 2\delta(\Delta H)], \tag{9}$$

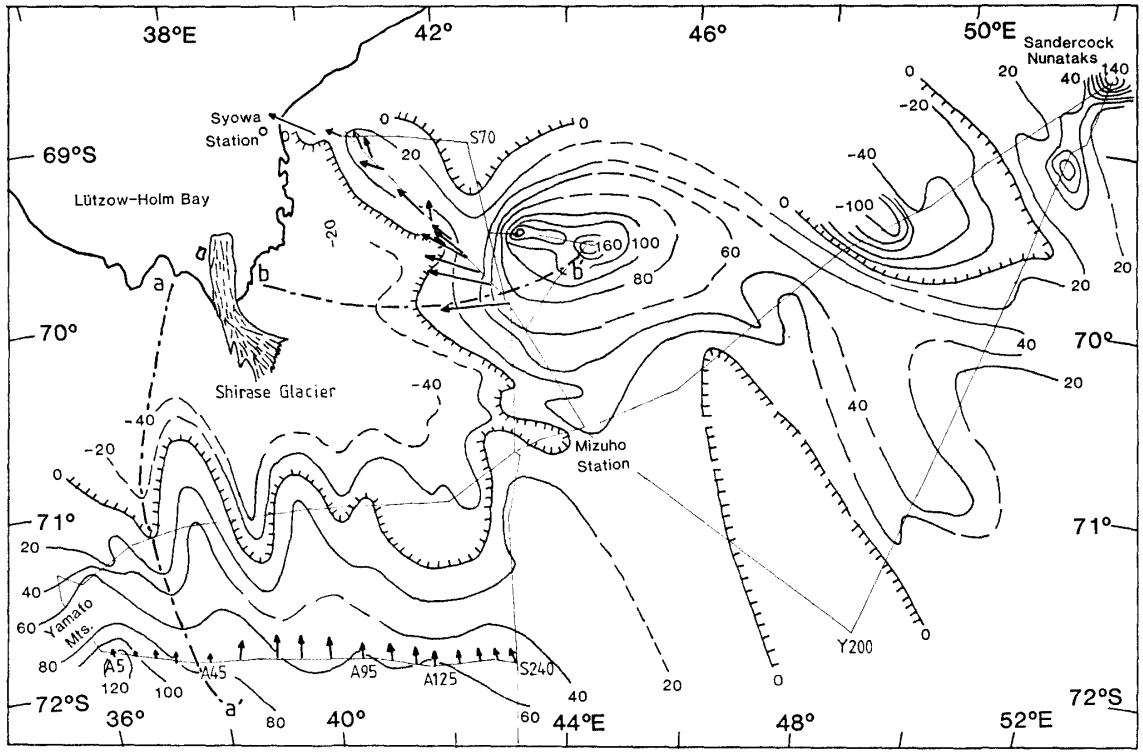

Fig. 7. Flow velocities on the S-H-Z and A routes superposed onto the free-air gravity anomaly map of the Mizuho Plateau reproduced from ABE et al.'s paper (1978) by the authors' courtesy.

where ΔH is the deviation of the elevation of bedrock from a standard value. Equation (9) is an approximation based on appropriate density contrast of bedrock to ice. If the representative slope of the ice sheet surface is taken to be $5-20\times10^{-3}$ over the Sôya drainage basin, the change of height δh in a horizontal distance of 20 km is 100–400 m. If the free-air anomaly $\delta(\Delta g_o)$ changes 20–40 mgal in a distance of 20 km as usually observed on the S-H-Z route for the direction of the maximum slope of the contours, the relative elevation of bedrock relief $\delta(\Delta H)$ is calculated by eq. (9) as 210–480 m or 70–330 m corresponding to the slope of 5×10^{-3} or 20×10^{-3}, respectively. If we adopt the representative value of 300 m as the bedrock elevation which corresponds to a 20 mgal increase in free-air anomalies, an eye of 0–160 mgal contours in the central upper part of Fig. 7 roughly gives a subglacial mound of 2400 m in height. The obtained flow direction on the second portion of the S-H-Z route is in general agreement with the direction of the maximum slope of such subglacial mound.

An empirical formula as follows was proposed by NARUSE (1978) for the flow velocity V_s as a function of the surface inclination θ_s and the thickness of ice I.

$$V_s \sim 0.83\ (\sin\theta_s)^2\ I^3. \tag{10}$$

It was assumed in the derivation that the laminar flow without bed sliding took place. According to eq. (10), the surface flow velocity in the neighboring region of the S-H-Z route are estimated as 9 ma^{-1} at S30, 12 ma^{-1} at S120 and 16 ma^{-1} at Z35, respectively (after Table 3 of NARUSE and SHIMIZU, 1978). However, the velocity in Table 6 ob-

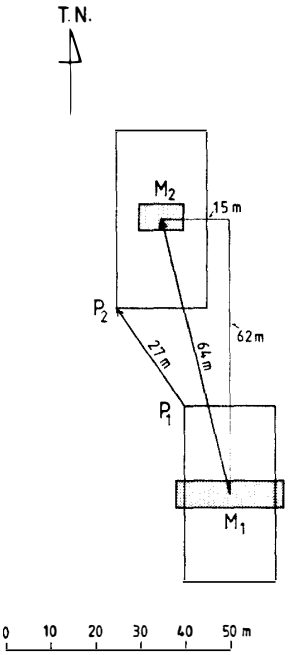

Fig. 8. The change of the NNSS-receiving position which is reduced to T109 (Mizuho Station) in 1.1 year between 1979–1980.

served in the present study ranges from 15 ma^{-1} at S27-3 to 67 ma^{-1} at Z2. Especially, the observed velocity at Z2 is as large as three times the above estimate, even if $\pm 14\%$ error is taken into consideration. We do not know yet the real reason of the discrepancy between the estimated and the observed values, but the former might be underestimated.

An estimate of the flow velocity by the direct comparison of NNSS positioning results can only be made at Mizuho Station where JARE-20 and -21 carried out the NNSS positioning at the same location using the same receiver JMR-1 under similar receiving conditions. Figure 8 shows the change of the position in a period between October 1979 and November 1980, from M_1 in 1979 (see Table 6 in a paper by the MEMBERS OF THE YAMATO-BELGICA TRAVERSE PARTY, 1981) to M_2 in 1980 (see ST27 in Table 4). Receiver position moved 62 m northward and 15 m westward in a time interval of 1.1 year. The standard deviation areas were given by the shaded boxes around M_1 and M_2 in Fig. 8. However, larger uncertainty areas of open boxes have to be considered here taking the repeatability of the NNSS positioning by the broadcasted ephemerides into account. Even if we consider such a large uncertainty, more than 25 ma^{-1} surface velocity can be obtained as illustrated by $\overrightarrow{P_1P_2}$ in Fig. 8.

Larger observed velocity of flow in the area of the Sôya drainage basin than that estimated by eq. (10) may indicate that the sliding at the bottom of ice sheet takes place there. In such a case, the bedrock topography as indicated by free-air gravity anomaly in Fig. 7 may influence the pattern of flow. However, since V_s in eq. (10) depends upon θ_s by a second power and upon I in a third power, precise measurements of both the surface topography and the thickness of ice are necessary before determining whether the sliding at the bottom really takes place or not.

From the operational point of view on the snow field, Antarctic ice sheet can be considered as the sea of ice and the NNSS positioning is expected to be a powerful tool

for navigations on it. Besides this function for the navigation, the NNSS positioning can provide us an important information on the flow velocity if it is used for the positioning of registered bamboo poles along the traverse route which were maintained by continuous efforts of every oversnow traverse party. However, it is rather difficult to remove 10 m inaccuracy in case of a single-site NNSS positioning by the broadcasted ephemerides from the uncertainty of orbital information. In order to extract the continuous traces of the surface flow of the ice sheet, frequent NNSS-translocation of the traverse pole on the ice sheet as referred to the surveyed fixed point will be required in a long-term receiving experiment.

Acknowledgments

The authors express their sincere gratitude to Drs. S. KAWAGUCHI and A. IKAMI and all the members of JARE-21 for their encouragement during the field operations and wintering. They also thank Dr. R. NARUSE and Mr. Y. ABE for their valuable comments on the manuscript, and for their kindness in supplying unpublished data on the geodetic control for the estimate of errors. They are indebted to Prof. A. HIGASHI for critically reading and improving the manuscript. This research was partly financed by the budget for JARE, entitled "Geophysical investigation of the crust and upper-mantle structure around Syowa Station, East Antarctica (representative: T. NAGATA)". Calculations were made by HITAC M160II at the National Institute of Polar Research.

References

ABE, Y., YOSHIMURA, A. and NARUSE, R. (1978): Gravity anomalies and bedrock relief in Mizuho Plateau. Mem. Natl Inst. Polar Res., Spec. Issue, **7**, 37–43.

BOMFORD, B. G. (1980): Geodesy. 4th ed. Oxford, Oxford Univ. Press, 855p.

HEISKANEN, W. A. and MORITZ, H. (1967): Physical Geodesy. San Francisco, W. H. Freeman, 364p.

HUBENY, K. (1959): Weiterentwicklung der Gauss'schen Mittelbreiten-formeln. Z. Vermess., **84**, 159–163.

IKAMI, A., ITO, K., SHIBUYA, K. and KAMINUMA, K. (1982): Crustal structure of the Mizuho Plateau, Antarctica revealed by explosion seismology. Fourth International Symposium on Antarctic Earth Sciences, August 1982, Volume of Abstracts, comp. and ed. by P. R. JAMES *et al.* Adelaide, Univ. Adelaide, 87.

MEMBERS OF THE YAMATO-BELGICA TRAVERSE PARTY (1981): Dai-20-ji Nankyoku Chiiki Kansokutai Yamato·Berujika ryôkô hôkoku (Report of the Yamato-Belgica traverse by the 20th Japanese Antarctic Research Expedition in 1979–1980 field season). Nankyoku Shiryô (Antarct. Rec.), **73**, 210–245.

NARUSE, R. (1978): Studies on the ice sheet flow and local mass budget in Mizuho Plateau, Antarctica. Contrib. Inst. Low Temp. Sci., Hokkaido Univ., Ser. A, **28**, 1–54.

NARUSE, R. and YOKOYAMA, K. (1975): Position, elevation and ice thickness of stations. JARE Data Rep., **28** (Glaciol.), 7–47.

NARUSE, R. and SHIMIZU, H. (1978): Flow line of the ice sheet over Mizuho Plateau. Mem. Natl Inst. Polar Res., Spec. Issue, **7**, 227–234.

SHIBUYA, K., ITO, K. and KAMINUMA, K. (1982): Utilization of an NNSS receiver in the explosion seismic experiments on the Prince Olav Coast, East Antarctica, 2. Positioning. Nankyoku Shiryô (Antarct. Rec.), **76**, 73–88.

(Received April 4, 1983; Revised manuscript received June 3, 1983)